Journal of Electrochemistry

Volume 23
Issue 2 *Special Issue in Honor of Professor Zhaowu Tian on His 90th Birthday*

2017-04-28

Impact of Nafion Loading and Anion Adsorption on the Synthesis of Pt Monolayer Core-shell Catalysts

Lijun Yang

Dustin Banham

Elod Gyenge

Siyu Ye
Ballard Power Systems, 9000 Glenlyon Parkway, Burnaby, BC, V5J 5J8 Canada;, siyu.ye@ballard.com

DOI: 10.13208/j.electrochem.161243 **Artical ID**:1006-3471(2017)02-0170-10
Cite this: *J. Electrochem.* **2017**, *23*(2): 170-179 **Http**://electrochem.xmu.edu.cn

Impact of Nafion Loading and Anion Adsorption on the Synthesis of Pt Monolayer Core-Shell Catalysts

Lijun Yang[1,2], Dustin Banham[1], Elod Gyenge[2], Siyu Ye[1*]
(1. *Ballard Power Systems*, 9000 *Glenlyon Parkway*, *Burnaby*, *BC*, V5J 5J8 *Canada*; 2. *Department of Chemical and Biological Engineering*, *University of British Columbia*, 2360 *East Mall*,*Vancouver*, *British Columbia*, V6T 1Z3, *Canada*)

Abstract: Carbon supported palladium (Pd) nanoparticles were used as a model core material for the synthesis of platinum (Pt) monolayer core-shell catalysts using rotating disk electrode method and a copper (Cu) under potential deposition technique. The impact of Nafion on the synthesis process was revealed by electrochemical testing with various Nafion contents. The existence of Nafion influenced the Cu under potential deposition, galvanic replacement and eventually the oxygen reduction reaction activity of the core-shell catalyst. However, as long as the Nafion content was less than 5wt% in the test film, adding Nafion could help to bind catalyst onto the surface of electrode while maintaining promising catalytic activity. Unique anion adsorption/desorption peaks were observed on the surface of Pd in H_2SO_4 solution, which turned out to be an useful indicator to evaluate the impact of Nafion on the synthesis of the core-shell catalysts.

Key words: core-shell catalyst; oxygen reduction reaction; copper under potential deposition; Nafion content; anions adsorption
CLC Number: O646 **Document Code**: A

Significant progress has been made during the last 25 years in the research and development of fuel cells that has enabled the commercialization of fuel cell electric vehicles and other applications. However, further cost reduction is still required to support wide-spread commercialization of fuel cells. For polymer electrolyte membrane fuel cells (PEMFCs), the catalyst remains a major cost factor due to the use of platinum group metals (PGMs). In order to meet the commercial requirements of the catalyst for oxygen reduction reaction (ORR), several strategies [1-3] have been attempted to increase the utilization of Pt and the inherent activity per active site for Pt-based catalysts.

Recently, core-shell structured catalysts demonstrated promising ORR activities, due to their higher surface area and improved catalytic activity than commercial Pt/C catalyst. The favorable ORR activity of core-shell catalysts relates to both electronic and geometric effects introduced by the core materials to the Pt shell[4-6]. For example, Pt core-shell catalyst using Ti-Au as core has a mass activity up to 3 $A \cdot mg_{Pt}^{-1}$ and an unchanged ORR activity after 10,000 cycles based on rotating disk electrode (RDE) testing[7]. Pt monolayer (Pt_{ML}) catalyst on a PdAu alloy core showed only 8% performance loss after 100,000 cycles between 0.6 ~ 1 V in MEA testing[8].

Besides the choice of core materials, the thickness of the Pt shell and the quality of shell coverage are also believed to affect both the activity and durability of core-shell catalysts[9-10]. A controllable way to deposit a Pt_{ML} shell on top of the other metal (or metal alloy) cores is to use copper under-potential deposition (Cu UPD) and sequentially galvanic replacement[11]. Using RDE and electrochemical testing, the synthesis procedure and the ORR performance of Pt_{ML} core-shell catalysts can be easily investigated to fundamentally explore the novel Pt_{ML} core-shell catalysts.

Binder is required in the ink formula to adhere the catalyst onto the surface of the RDE. Either

Received: 2016-12-01, Revised: 2017-02-28 *Corresponding author, Tel: 01-604-4124778, E-mail: siyu.ye@ballard.com

Nafion ionomer or Triton nonionic surfactant can be used as binder for RDE testing, with Nafion being the most common binder of the two. However, it has been recently reported in the literature that strong an ion binding can occur between Nafion and PGM catalysts[12-13]. As the Cu UPD and galvanic replacement for the core-shell catalyst synthesis are occurring on the surface of metal cores, it appears likely that the existence of Nafion in RDE films could impact the process. In this work, we varied the Nafion loadings (from 0wt% to 30wt%) in the film, in order to explore the impact of Nafion loading to the synthesis process and eventually the activity of catalyst. We chose Pd as the model core since Pt-Pd core-shell catalysts have already been well studied so that significant data are available for comparison. It is clear that the discussion here can be extended to the other core materials, which might provide different catalytic performances.

We discovered unexpected adsorption/desorption peaks in the HUPD (hydrogen under potential deposition) region on the surface of polycrystalline Pd in H_2SO_4 solution (not in $HClO_4$) when the Nafion loading was decreased. Therefore, we wanted to understand if this is a unique phenomenon on Pd relating to the adsorption of sulfate/bisulfate anions. The surface electrochemical properties of Pd were also compared in less adsorptive $HClO_4$ to detect the influence of anion adsorption in the core-shell catalyst preparation procedure.

1 Experimental

20wt% Pd nanoparticle supported on Vulcan carbon (Premetek Co.) was used. These catalyst particles were mixed with MilliQ ultra-pure water (Millipore) and various amounts of 5.4wt% Nafion Alcoholic Polymer Dispersion (DuPont), followed by water bath ultra-sound sonication for 30 min to get a well dispersed ink. The ink formula was 3 mg of 20wt% Pd/C catalysts, x μL of 5.4wt% Nafion dispersion and (3000-x) μL of H_2O. The x was the value calculated according to the Nafion content in the final dried film comprised of Nafion and Pd/C catalyst. The density of 5.4wt% Nafion dispersion was 0.915 $g \cdot cm^{-3}$. In this study, we varied Nafion contents to 0, 5, 10, 15 and 30wt%, thus, the x values were 0, 3.2, 6.8, 10.8 and 26.1, respectively. After sonication, 20 μL of the ink slurry was pipetted onto the surface of glassy carbon rotation disk electrode (RDE) with a diameter of 5 mm (area: 0.196 cm^2). That is, the Pd loading was 20.4 $\mu g \cdot cm^{-2}$ on RDE. Before every experiment, the RDE was polished by 0.05 μm Al_2O_3 powder, sonication cleaned and raised thoroughly with ultra-pure H_2O to get clean and smooth surface. To indicate the content of Nafion on RDE, we use a simplified notation. For example, Pd/C-5Naf denotes Pd/C catalysts with a finally 5wt% Nafion in the film on RDE.

The electrochemical evaluations and preparations of Pt_{ML}-Pd core-shell catalysts were performed in a three-electrode cell by the control of potentiostat (Model 263A, Princeton Applied Research). Pd/C loaded RDE was the working electrode, Pt wire was the counter electrode, while reversible hydrogen electrode (RHE) was the reference electrode.

Firstly, the cyclic voltammetric (CV) curves of Pd/C with various Nafion contents were tested in either 0.05 $mol \cdot L^{-1}$ H_2SO_4 solution or 0.1 $mol \cdot L^{-1}$ $HClO_4$ solution with/without adding 0.05 $mol \cdot L^{-1}$ K_2SO_4. The solutions were purged with N_2 for at least 30 min before every test. 20 cycles of CV curves were recorded with a scan rate of 20 $mV \cdot s^{-1}$. The reported CV curves in this study were the last cycle from each catalyst.

Secondly, the working electrodes were kept at 0.2 V for 2 min to reduce the surface oxides on Pd that probably produced during the CV cycles. After that, each Pd/C with various Nafion contents went through a Cu UPD followed by a galvanic replacement to obtain Pt monolayer on top of the Pd. The procedure was as follows: 1) In 0.05 $mol \cdot L^{-1}$ H_2SO_4 + 0.05 $mol \cdot L^{-1}$ $CuSO_4$ solutions, the CV curve of Cu UPD on Pd/C was taken in the region of 0.35 V ~ 0.75 V with the scan rate of 20 $mV \cdot s^{-1}$. The purpose of this CV scan was to roughly determine the potential of Cu UPD on Pd/C catalysts while avoiding the possible oxidation of Pd; 2) Linear sweep voltammetry was applied on the working electrode from 0.75 V

with the scan rate of 5 mV·s^{-1}. When the potential reached the value that Cu UPD finished (the position investigated on Step 1), it was held for 2 min to enable the Cu UPD being fully processed and Cu_{ML}-Pd/C was obtained; 3) The Cu_{ML}-Pd/C was immersed in 0.05 mol·L^{-1} H_2SO_4 + 1 mmol·L^{-1} K_2PtCl_4 solutions for 10 min to allow replacement between Pt^{2+} and Cu monolayer, and the open circuit potential (OCP) was recorded during the replacement.

Finally, the as-prepared Pt_{ML}-Pd/C catalysts with various Nafion contents were evaluated in both N_2 purged and O_2 saturated 0.1 mol·L^{-1} $HClO_4$. The oxygen reduction reaction (ORR) currents were obtained from the anodic scan in O_2 saturated 0.1 mol·L^{-1} $HClO_4$, subtracting the non-Faradic currents obtained in N_2 purged solution. For the purpose of comparison, the CV curves of Pt_{ML}-Pd/C catalysts in N_2 purged 0.05 mol·L^{-1} H_2SO_4 solution were also recorded.

2 Results and Discussion

The theory and procedure of preparing Pt_{ML}-Pd core-shell catalysts through Cu UPD and sequential galvanic replacement have been described in several publications[11, 14]. As shown in Figure 1A, the general process is as follows:

1) Cu UPD on Pd

Cu monolayer on Pd (Cu_{ML}-Pd) can be obtained by precisely control of the deposition voltage on Pd in 0.05 mol·L^{-1} H_2SO_4 + 0.05 mol·L^{-1} $CuSO_4$ solutions. The amount (mol) of deposited Cu can be calculated from the integrated charge of Cu UPD, according to Faraday's Law, $n = Q/(zF)$, n is the mol of Cu deposited on Pd; Q is the integrated charge for Cu UPD; z is the number of electrons involved in the reaction, which is 2 in this case; F is the Faraday constant, which is 96485.

2) Galvanic Replacement

Cu monolayer on Cu_{ML}-Pd is replaced by Pt in 0.05 mol·L^{-1} H_2SO_4 + 1 mmol·L^{-1} K_2PtCl_4 solutions to form a Pt monolayer on Pd (Pt_{ML}-Pd), following the reaction of Pt^{2+} + Cu → Pt + Cu^{2+}. The driving force for this replacement reaction is the standard redox potential difference between Cu^{2+}/Cu (0.34 V) and Pt^{2+}/Pt (1.18 V). The open circuit potential (OCP) of the working electrode is monitored during replacement in order to get information related to the dissolution of Cu and the formation of Pt monolayer.

In this study, Vulcan carbon supported Pd nanoparticles (mean particle size of 4 ± 0.2 nm) were the core material used to prepare core-shell catalysts. With or without the addition of Nafion, the surface environment of Pd particles could be different. As shown in Figure 1B, if Nafion is added, there might

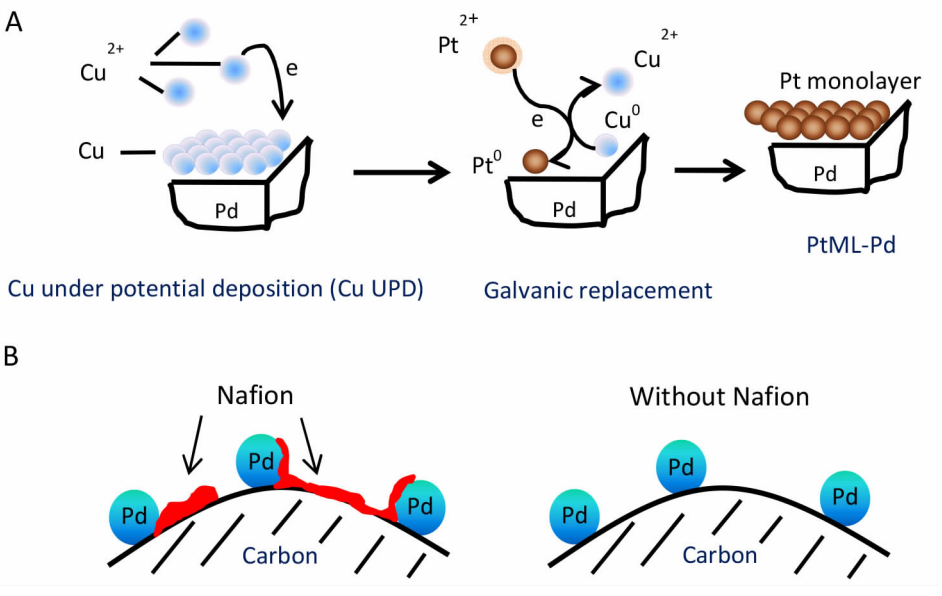

Fig. 1 A. Schematic process for the preparation of Pt_{ML}-Pd core-shell catalyst by Cu under potential deposition and galvanic replacement[15]; B. Two possible surface situations of the Pd/C catalyst: with or without Nafion added in the ink

be a discontinuous Nafion coating either on the Pd particles or on the carbon support, and the coverage of Nafion on Pd and/or carbon increases with the Nafion content. If there is no Nafion, the surface of poly-crystalline palladium is exposed.

2.1 Impacts of Anion Adsorption and Nafion Content on the Surface of Pd/C

Before preparation of core-shell catalysts, the surface properties of Pd/C without adding Nafion were evaluated, as shown in Figure 2. Comparing the CV curves in 0.05 mol·L^{-1} H_2SO_4 and 0.1 mol·L^{-1} $HClO_4$ solutions with/without adding K_2SO_4, one can conclude that the existence of SO_4^{2-}/HSO_4^- anions brings two effects to the surface of Pd: 1) It delayed the onset of PdO/PdOH formation on Pd, which is due to the much stronger adsorption strength of SO_4^{2-}/HSO_4^- anion on the surface of Pd compare to ClO_4^-[16]. 2) It introduced two pairs of sharp butterfly shaped peaks in the region of 0.1 ~ 0.3 V. According to single crystal studies, the SO_4^{2-}/HSO_4^- anion adsorption/desorption on the surface of Pd could generate charge in the range of 0.2 ~ 0.3 V, which overlays with the HUPD on Pd[17-18]. The butterfly shaped peaks probably relate to both the adsorption/desorption of SO_4^{2-}/HSO_4^- as well as H on the surface of Pd. Nevertheless, these sharp peaks could be useful indicators

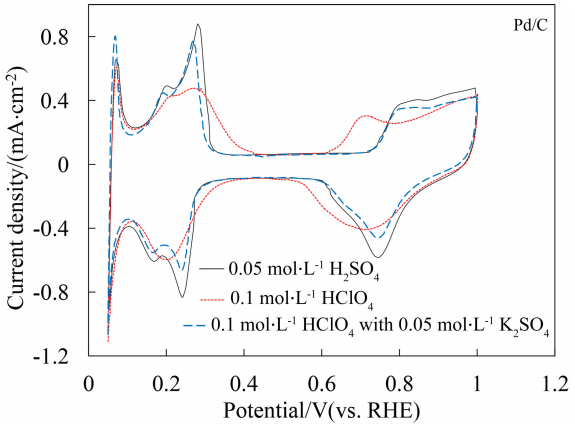

Fig. 2 Cyclic voltammetric curves of 20% Pd/C catalyst without Nafion in N_2 purged 0.05 mol·L^{-1} H_2SO_4 solution, 0.1 mol·L^{-1} $HClO_4$ solution and 0.1 mol·L^{-1} $HClO_4$ solution containing 0.05 mol·L^{-1} K_2SO_4. The scan rate was 20 mV·s^{-1}.

to investigate the impact of Nafion on the surface properties of Pd.

The CV curves of Pd/C with various Nafion contents in 0.1 mol·L^{-1} $HClO_4$ and 0.05 mol·L^{-1} H_2SO_4 solutions were studied. In 0.1 mol·L^{-1} $HClO_4$ solution (not shown here), the CVs of the catalysts showed almost no change with Nafion content in the studied voltage region. Conversely, the CVs in 0.05 mol·L^{-1} H_2SO_4 solution (Figure 3) presented some interesting characteristics. With the increase of Nafion content from 0 to 30wt%, there were two major changes:

1) 0.1 ~ 0.3 V: the butterfly shaped peaks gradually decreased with increasing of Nafion content, except for Pd/C-5Naf which had similar peaks to Pd/C-0Naf. According to the hypothesis of adsorption/desorption of SO_4^{2-}/HSO_4^- on Pd/C, the decrease of the sharp peaks can be assigned to less contribution from SO_4^{2-}/HSO_4^- anion adsorption/desorption charges. Alternatively, Nafion may also adsorb on Pd through its SO_3^- groups[19]. When the Nafion loading is high enough, it may compete with SO_4^{2-} and suppress SO_4^{2-} adsorption on Pd in the HUPD region.

2) 0.6 ~ 1 V: the peak areas of Pd-O/Pd-OH formation decreased with increasing Nafion content. In addition, at 30wt% Nafion, a large anodic voltage shift could be noticed. It is believed that the additional Nafion adsorption could delay the onset of the oxidation of Pd by H_2O[20].

In conclusion, the existence of Nafion in Pd/C catalyst film might influence the strong SO_4^{2-}/HSO_4^- anion adsorption/desorption and surface oxidation on Pd. However, when the Nafion content went as low as 5wt%, the impact could be almost eliminated.

2.2 Impact from Nafion Content to the Preparation of Pt_{ML}-Pd Core-Shell Catalysts

The CV curves on 20wt% Pd/C were investigated in N_2 purged 0.05 mol·L^{-1} H_2SO_4 + 0.05 mol·L^{-1} $CuSO_4$ solutions. For clarity, three CVs are presented in Figure 4. The scan region was set between 0.35 V ~ 0.75 V vs. RHE to avoid interference from HUPD, Cu bulk deposition and reduction charge from Pd-O/Pd-OH[21]. Pd/C-0Naf showed a typical Cu UPD (ca-

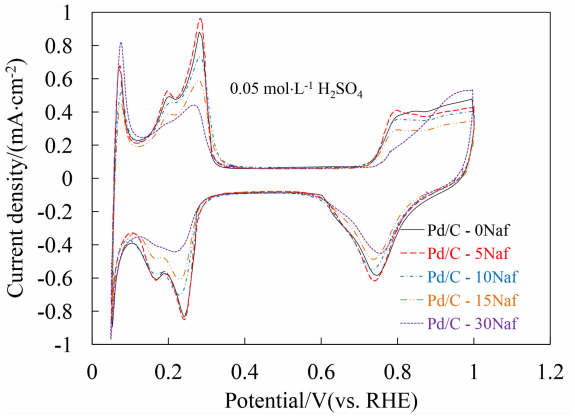

Fig. 3 Cyclic voltammetriccurves of 20% Pd/C with various Nafion loadings in N_2 purged 0.05 mol·L^{-1} H_2SO_4 solution under a scan rate of 20 mV·s^{-1}

thodic scan) and stripping (anodic scan) process. There were at least six cathodic peaks on polycrystalline Pd, corresponding to six adsorption steps of Cu adatoms onto different Pd crystalline planes[22-23]. As the Nafion content increased, the Cu UPD peaks in the potential region of 0.45 V ~ 0.65 V were gradually decreased, while the peak on ~0.37 V was enlarged. The adsorption of Nafion on Pd might alter the adsorption strength of Cu atoms onto Pd and this could change the shape of Cu UPD peaks. As listed in Figure 4, the integrated charges of Cu UPD peaks (before bulk Cu deposition) from the five samples could be grouped

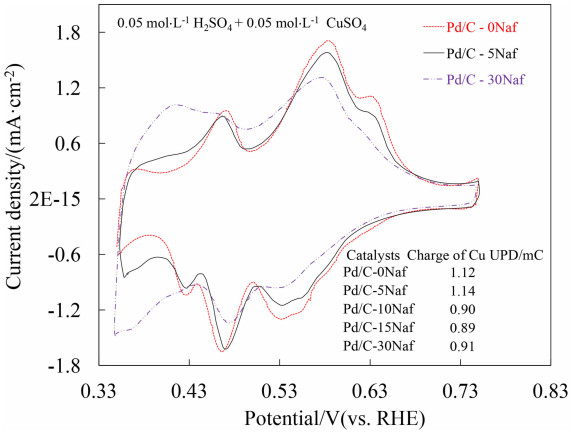

Fig. 4 Cyclic voltammetric curves of 20% Pd/C with 0, 5 and 30wt% Nafion in N_2 purged 0.05 mol·L^{-1} H_2SO_4 + 0.05 mol·L^{-1} $CuSO_4$ solutions under a scan rate of 20 mV·s^{-1}. The integrated charges of Cu UPD on Pd/C with various Nafion loadings are listed in the graph.

into two. One group was 0Naf and 5Naf, the values were ~ 1.1 mC and they were close to the value of one monolayer of Cu on top of Pd (if we took the charge value of 402 μC·cm^{-2}[24] for a 1:1 Cu to Pd atom ratio, while using the mean particle size of 4 nm for Pd nanoparticles to calculate the surface area of Pd). The other group was 10Naf, 15Naf and 30Naf, for which the Cu UPD charges were 20% less than Group one, meaning that there were less Cu atoms deposited on Pd at these higher Nafion contents.

After the Cu monolayer was obtained on Pd/C, the electrode with Cu_{ML}-Pd/C was immersed into a 0.05 mol·L^{-1} H_2SO_4 solution containing 1 mmol·L^{-1} K_2PtCl_4, for the process of galvanic replacement to form a Pt monolayer on Pd/C. The OCP was recorded once the electrode was immersed into the solution. OCP is the mixed potential value from reactions on the surface of Cu, Pd or Pt, and should gradually increase when Cu was being replaced by Pt on top of Pd. Therefore, a plot of OCP vs. time can be used as an *in-situ* indicator to investigate the impact of Nafion content on the galvanic replacement. As shown in Figure 5, the evolution of OCP contained two phases, one was the rapid increase, and the other was the slow increase until a stable plateau was reached. Both of the phases were impacted by Nafion content. For different Nafion contents, the OCP vs. time curves could be divided into 2 groups: 1) 0Naf

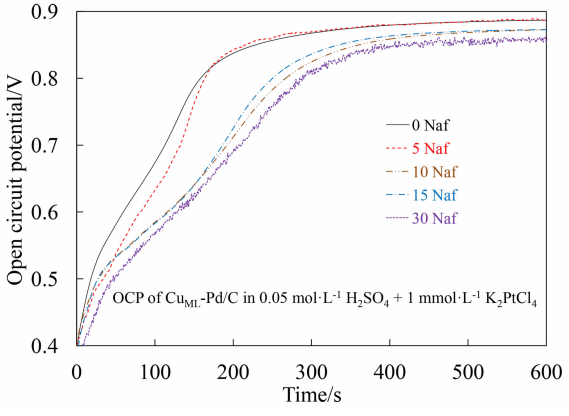

Fig . 5 Plotted curves of open circuit potential (OCP) vs. time on Cu_{ML}-Pd/C with various Nafion loadings in N_2 purged 0.05 mol·L^{-1} H_2SO_4 + 1 mmol·L^{-1} K_2PtCl_4 solution

and 5Naf, and 2) 15-30 Naf.

Goup 1, 0Naf and 5Naf, had fast OCP increase rate, and the final plateau in OCP reached a higher value than Group 2. Compared to Group 1, the rate of OCP increase on 10Naf-30Naf was slower. It took around 2 min more for the OCP to reach a plateau that was 15 mV lower than that of Group 1. It is likely that the presence of Nafion on the surface of Pd hindered both the diffusion of Pt^{2+} and the departure of Cu^{2+}, eventually delaying the reaction rate of galvanic replacement. The higher the Nafion content was, the more the reaction was impacted. Additionally, the final OCP values decreased with increasing Nafion content, possibly due to the Pt shell quality (continuous coverage) on Pd being less perfect with the increase in Nafion content, as the OCP of Pt in H_2SO_4 was higher than the Pd[25-26].

All of the as-prepared Pt_{ML}-Pd/C catalysts were cleaned with H_2O, and their ORR activity was evaluated in either 0.05 mol·L^{-1} H_2SO_4 or 0.1 mol·L^{-1} $HClO_4$ solution. During this process, it was observed that part of the catalysts without Nafion (Pt_{ML}-Pd/C-0Naf) detached from the RDE since there was little affinity between catalysts and the RDE surface (glassy carbon). For the purpose of comparison, the CV curve of Pt_{ML}-Pd/C -0Naf is still presented with the other catalysts prepared with different Nafion contents. However, it is difficult to accurately estimate the Pt mass activity of Pt_{ML}-Pd/C -0Naf for the ORR. We used the charge of the Cu UPD to calculate the amount of Pt in the catalyst, although it was clear that a part of the Pt_{ML}-Pd/C-0Naf catalyst was lost after Cu UPD and galvanic replacement.

Figure 6 shows the CV curves of the Pt_{ML}-Pd/C core-shell catalysts with various Nafion contents in 0.05 mol·L^{-1} H_2SO_4 solution. It is obvious that both the HUPD current and double layer of the Pt_{ML}-Pd/C -0Naf were smaller than all the other catalysts, which provides evidence that some of this catalyst was de tached from the electrode. According to previous data (shown in Figures 3 and 4), the Pt_{ML}-Pd/C-0Naf and Pt_{ML}-Pd/C -5Naf should have quite similar double layer capacitance since the loading of Pd/C, Cu UPD charges and Pt replacement trend were close between these two. If we compared the double layer capacitances in Figure 6, at least 44% of Pt_{ML}-Pd/C-0Naf had detached from the electrode. For the catalysts with Nafion addition, the content of Nafion had several impacts: 1) The H UPD current and surface oxidation/reduction current on Pt_{ML}-Pd/C catalysts decreased with increasing Nafion content, indicating a decrease of surface area and/or Pt loading of Pt_{ML}-Pd/C with an increase of Nafion content; 2) For Pt_{ML}-Pd/C -10Naf and Pt_{ML}-Pd/C-15Naf, there was one small peak at 0.25 V, which sat at the same position as the butterfly shaped peaks on Pd. This could indicate an incomplete coverage of Pt on the Pd nanoparticles meaning that part of the surface of Pd was exposed to electrolyte, allowing for anion adsorption to take place on the surface of Pd. Additionally, incomplete coverage of the Pd would allow for proton absorption onto the Pd core resulting in a larger charge than expected in the HUPD region; 3) For Pt_{ML}-Pd/C -30Naf, the charges in HUPD region and surface oxides formation region on the catalyst were much smaller than the samples with other Nafion contents. This might not only due to the lower Pt coverage on Pd, but also the influence of Nafion adsorption to the CV behaviors at the surfaces of the core-shell catalyst. In conclusion, Pt_{ML}-Pd/C-5Naf showed the best trade-off between adhesion and active site blocking.

In order to investigate the impacts of anions on

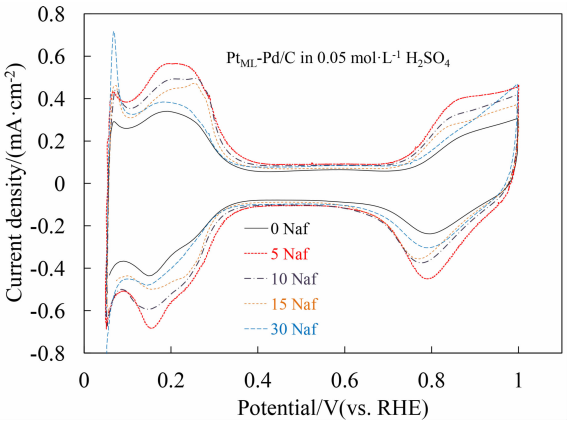

Fig. 6 Cyclic voltammetriccurves of prepared Pt_{ML}-Pd/C with various Nafion loadings in N_2 purged 0.05 mol·L^{-1} H_2SO_4 solution under a scan rate of 20 mV·s^{-1}

the surface properties of Pd/C and Pt_{ML}-Pd/C catalyst, the CV curves of Pd/C before and after depositing Pt monolayer in both 0.05 mol·L^{-1} H_2SO_4 and 0.1 mol·L^{-1} $HClO_4$ solutions are compared. The 5wt% Nafion content sample is presented in Figure 7A and 7B. For both electrolytes, the Pd/C and Pt_{ML}-Pd/C showed quite different HUPD and surface oxides formation behaviors. This was actually a clear indicator to show the formation of a Pt monolayer on top of Pd through this preparation method, as Pd and Pt monolayer have different surface responses to HUPD and oxidation with the electrolytes[27-28]. The distinction between Pd/C and Pt_{ML}-Pd/C was more obvious in 0.05 mol·L^{-1} H_2SO_4 solution than in 0.1 mol·L^{-1} $HClO_4$ solution. As mentioned previously, the butterfly shaped peaks in the region of 0.1 ~ 0.3 V might relate to the adsorption/desorption of SO_4^{2-}/HSO_4^- on Pd. They vanished after Pt monolayer depositedon the Pd nanoparticle, since the adsorption/desorption of SO_4^{2-}/HSO_4^- were reported to be weaker on Pt than on Pd in this particular voltage region[19]. Additionally, there was a notable current increase in the double layer region (0.3 ~ 0.7 V) on Pt_{ML}-Pd/C compared to Pd/C in 0.05 mol·L^{-1} H_2SO_4. According to literature[17, 29], SO_4^{2-}/HSO_4^- started to adsorb on the surface of Pt around 0.3 V. The adsorption/desorption of SO_4^{2-}/HSO_4^- on Pt mono-layer might contribute to this particular increase in charge in the double layer region.

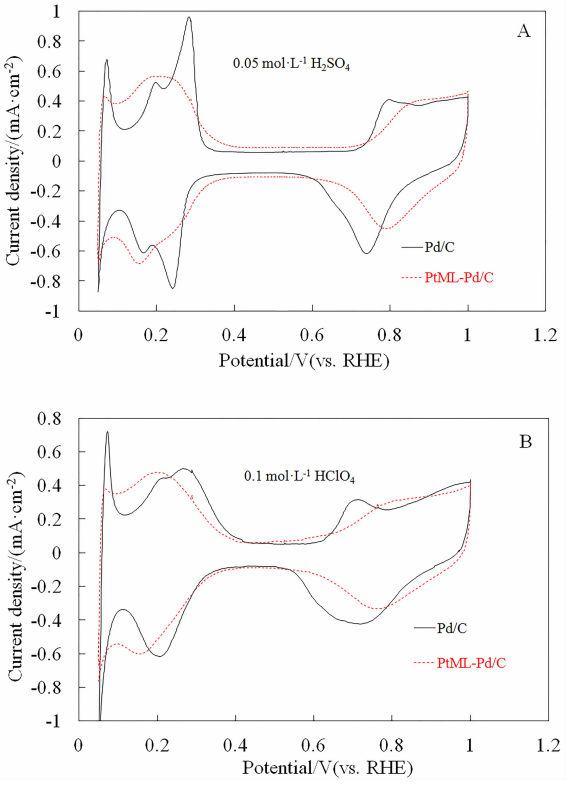

Fig. 7 Comparison of CV curves on Pt_{ML}-Pd/C-5Naf and Pd/C-5Naf in N_2 purged (A) 0.05 mol·L^{-1} H_2SO_4 and (B) 0.1 mol·L^{-1} $HClO_4$ solutions under a scan rate of 20 mV·s^{-1}

The ORR polarization curves of Pt_{ML}-Pd/C with various Nafion contents were obtained by subtracting the CV curves in N_2 purged 0.1 mol·L^{-1} $HClO_4$ solutions from O_2 saturated ones. The current readings were from the anodic sweep. The i_k (mass-transport free kinetic current) is calculated after mass-transport correction[30]:

$$i_k = \frac{i_1 \times i}{i_1 - i} \quad (1)$$

where i_l is the diffusion-limited current and the i is the current read from polarization curves. The i_k vs. voltage curves are shown in Figure 8A. Since part of the Pt_{ML}-Pd/C-0Naf had detached from the RDE, it is not surprising that the ORR activity of the catalyst was lower than the other Pt_{ML}-Pd catalysts. Additionally, the Pt_{ML}-Pd/C catalysts with Nafion addition showed the ORR activities following the sequence of 5Naf ＞ 10Naf ＞15Naf ≈ 30Naf in the voltage region of 0.85 ~ 0.95 V vs. RHE. That is, the less Nafion was added in the original ink, the better ORR activity was on the Pt_{ML}-Pd/C catalyst. Calculated mass activity (kinetic current per Pt loading), as well as specific activity (kinetic current per Pt surface area) at 0.9 V (vs. RHE) are used as criteria to evaluate the ORR activity of the catalysts. For mass activity, the Cu UPD charge was used to calculate the Pt loading that couldbe deposited on Pd. As the case of Pt_{ML}-Pd/C- 0Naf, if we assumed 44% of the catalyst had fallen from the RDE (compare the double layer of the 0Naf and 5Naf ones), the calculated mass activity should be 0.89 A·mg^{-1}_{Pt} , that was very close to the reported data without the addition of Nafion[28]. Along with the increase of Nafion from 5 to 30wt%, the mass activi ty of Pt_{ML}-Pd/C decreased from 0.83 to 0.55

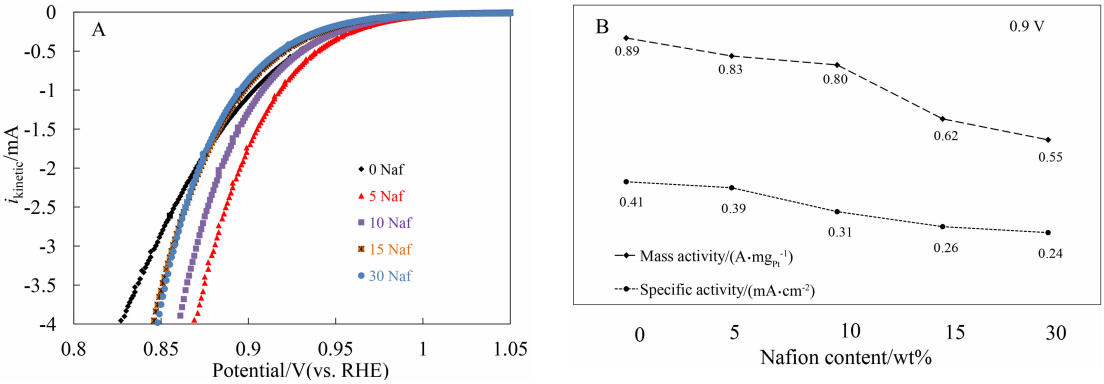

Fig. 8 A. ORR current of Pt_{ML}-Pd/C catalysts with various Nafion loadings obtained in O_2 saturated 0.1 mol·L^{-1} $HClO_4$ solution under a rotation speed of 1600 r·min^{-1}, the scan rate was 20 mV·s^{-1}; B. Calculated mass activities and specific activities for ORR at 0.9 V (vs. RHE) on the Pt_{ML}-Pd/C catalysts with various Nafion contents.

A·mg$^{-1}_{Pt}$. This could be a consequence from Nafion impacts on both Cu UPD and Pt galvanic replacement of Cu monolayer on the surface of Pd/C nanoparticles, as we observed before. For specific activity, the impact of Nafion content on ORR activity was similar. Pt_{ML}-Pd/C-0Naf had the highest activity (0.41 mA·cm$^{-2}_{Pt}$), Pt_{ML}-Pd/C-5Naf had slightly lower value (0.39 mA·cm$^{-2}_{Pt}$), while the value gradually decreased to 0.24 mA·cm$^{2}_{Pt}$ for Pt_{ML}-Pd/C-30Naf. Since the electrochemical surface area of Pt was calculated from H desorption peak on the final Pt_{ML}-Pd/C, the calculated values were reliable for all the samples including Pt_{ML}-Pd/C-0Naf.

Since Pd/C nanoparticles were used as the same core materials, there were two major factors for determining the ORR activity of Pt_{ML}-Pd/C catalysts in this work: 1) the quality of Pt shell on Pd, that is, the continuous coverage and the smoothness of the shell; and 2) total amount of accessible active sites for the ORR on the surface of catalysts. The presence of Nafion could impact both the Pt shell quality during the preparation and the accessibility of surface active sites of the catalyst as it could be adsorbed on the surface of Pd and Pt, and thus impacted the ORR activity of Pt_{ML}-Pd/C. As a result, the less Nafion that was added, the better ORR activity the Pt_{ML}-Pd/C catalysts possess. Comparing the ORR activity of Pt_{ML}-Pd/C-0Naf and Pt_{ML}-Pd/C-5Naf, the difference was less than 10%. Thus, as long as the Nafion content was ≤ 5wt% in the film, the properties of the core-shell catalyst was not significantly impacted.

3 Conclusions

For the purpose of preparing Pt_{ML}-Pd/C core-shell catalyst on RDE through Cu UPD technique, Nafion was used as a binder to prevent the catalyst from detaching from the surface of electrode. The impact of Nafion on the preparation of Pt_{ML}-Pd/C catalysts was investigated by varying the Nafion contents from 0 to 30wt%. The presence of Nafion altered the Cu UPD and galvanic replacement processes, and thus changed the ORR catalytic activities of the final catalysts. The 5wt% Nafion was found to be ideal, since it was successful in binding the catalyst to the glassy carbon surface, while having minimal impact on the preparation of the core-shell catalysts. However, for a large-scale preparation and long term development of core-shell catalysts, Nafion free synthesis methods should be considered and developed.

The CV curves of Pd/C and Pt_{ML}-Pd/C catalysts were evaluated in both non-adsorptive $HClO_4$ and adsorptive H_2SO_4 solutions to show the impacts of anion binding on the preparation of core-shell catalysts. The unique butterfly shaped peaks related to the adsorption/desorption of SO_4^{2-}/HSO_4^- on Pd and had a clear response to both the increasing Nafion content and the formation of a Pt monolayer. It could be a useful indicator to evaluate the impact of Nafion on the synthesis of core-shell catalysts.

Electrochemical evaluations were applied to reveal the impacts of Nafion and anion adsorption on

the synthesis of Pt-Pd core-shell catalysts. For the future work, the focus would be on relating the shell quality (or Pt coverage) to the catalytic activity of the core-shell catalysts. For that purpose, several characterization techniques can be used, such as scanning transmission electron microscopy (STEM), electron energy loss spectroscopy (EELS) and XRD under H_2/He environment.

Acknowledgements

Financial supports to Lijun Yang's post-doctoral fellowship by MITACS Accelerate Program and Ballard Power Systems are greatly appreciated. We also thank Julie Bellerive, Ping He, and Shanna Knights for many helpful discussions.

References:

[1] Wang Y J, Zhao N N, Fang B Z, et al. Carbon-supported Pt-based alloy electrocatalysts for the oxygen reduction reaction in polymer electrolyte membrane fuel cells: Particle size, shape, and composition manipulation and their impact to activity[J]. Chemical Reviews, 2015, 115(9): 3433-3467.

[2] Shao M H, Chang Q W, Dodelet J P, et al. Recent advances in electrocatalysts for oxygen reduction reaction[J]. Chemical Reviews, 2016, 116(6): 3594-3657.

[3] Zhang J, Li C M. Nanoporous metals: fabrication strategies and advanced electrochemical applications in catalysis, sensing and energy systems[J]. Chemical Society Reviews, 2012, 41(21): 7016-7031.

[4] Oezaslan, M, Hasche F, Strasser P. Pt-based core-shell catalyst architectures for oxygen fuel cell electrodes[J]. Journal of Physical Chemistry Letters, 2013, 4(19): 3273-3291.

[5] Wang X, Choi S I, Roling L T, et al. Palladium-platinum coreshell icosahedra with substantially enhanced activity and durability towards oxygen reduction[J]. Nature Com munications, 2015, 6: 7594.

[6] Zhao Z L, Zhang L Y, Bao S J, et al. One-pot synthesis of small and uniform Au@PtCu core-alloy shell nanoparticles as an efficient electrocatalyst for direct methanol fuel cells[J]. Applied Catalysis B: Environmental, 2015, 174: 361-366.

[7] Hu J, Wu L J, Kuttiyiel K A, et al. Increasing stability and activity of core-shell catalysts by preferential segregation of oxide on edges and vertexes: Oxygen reduction on Ti-Au@Pt/C[J]. Journal of the American Chemical Society, 2016, 138(29): 9294-9300.

[8] Sasaki K, Naohara H, Choi Y M, et al. Highly stable Pt monolayer on PdAu nanoparticle electrocatalysts for the oxygen reduction reaction[J]. Nature Communications, 2012, 3: 1115.

[9] Zhang L, Zhu S, Chang Q, et al. Palladium-platinum core-shell electrocatalysts for oxygen reduction reaction prepared with the assistance of citric acid[J]. ACS Catalysis, 2016, 6(6): 3428-3432.

[10] Cai Y, Adzic R R. Platinum monolayer electrocatalysts for the oxygen reduction reaction: Improvements induced by surface and subsurface modifications of cores[J]. Advances in Physical Chemistry, 2011: Article ID 530397.

[11] Yang L J, Vukmirovic M B, Su D, et al. Tuning the catalytic activity of Ru@Ptcore-shell nanoparticles for the oxygen reduction reaction by varying the shell thickness[J]. Journal of Physical Chemistry C, 2013, 117(4): 1748-1753.

[12] Shinozaki K, Zack J W, Pylypenko S, et al. Oxygen reduction reaction measurements on platinum electrocatalysts utilizing rotating disk electrode technique[J]. Journal of the Electrochemical Society, 2015, 162 (12): F1384-F1396.

[13] Zhu S, Hu, X, Zhang L, et al. Impacts of perchloric acid, nafion and alkali metal ions on oxygen reduction reaction kinetics in acidic and alkaline solutions[J]. The Journal of Physical Chemistry C, 2016, 120(48): 27452-27461.

[14] Vukmirovic M B, Bliznakov S T, Sasaki K, et al. Electrodeposition of metals in catalyst synthesis: The case of platinum monolayer electrocatalysts[J]. The Electrochemical Society Interface, 2011, 20(2): 33-40.

[15] Yang L J(杨莉君). Preparation and investigation of core-shell structured Pt monolayer catalysts and carbon based non-Pt catalysts[D]. Guangzhou: South China University of Technology(华南理工大学), 2013.

[16] Hara M, Linke U,Wandlowski T. Preparation and electrochemical characterization of palladium single crystal electrodes in 0.1 M H_2SO_4 and $HClO_4$ part I. Low-index phases[J]. Electrochimica Acta, 2007, 52(18): 5733-5748.

[17] Hoshi N, Kuroda M, KogaO, et al. Infrared reflection absorption spectroscopy of the sulfuric acid anion on low and high index planes of palladium[J]. The Journal of Physical Chemistry B, 2002, 106(35): 9107-9113.

[18] Hoshi N, Kagaya K,Hori Y.Voltammograms of the singlecrystal electrodes of palladium in aqueous sulfuric acid electrolyte: Pd(S)-[n(111)×(111)] and Pd(S)-[n(100)×(111)][J]. Journal of Electroanalytical Chemistry, 2000, 485(1): 55-60.

[19] Álvarez B, Climent V, RodesA, et al. Anion adsorption on Pd-Pt(111) electrodes in sulphuric acid solution[J].

Journal of Electroanalytical Chemistry, 2001, 497(1/2): 125-138.

[20] Ahmed M, Attard G A, Wright E, et al. Methanol and formic acid electrooxidation on nafion modified Pd/Pt {111}: The role of anion specific adsorption in electrocatalytic activity[J]. Catalysis Today, 2013, 202(1): 128-134.

[21] Kumar A, Buttry D A. Size-dependent underpotential de position of copper on palladium nanoparticles[J]. The Journal of Physical Chemistry C, 2015, 119(29): 16927-16933.

[22] Okada J, Inukai J, Itaya K. Underpotential and bulk deposition of copper on Pd(111) in sulfuric acid solution studied by *in situ* scanning tunneling microscopy[J]. Physical Chemistry Chemical Physics, 2001, 3(16): 3297-3302.

[23] Lenz P, Solomun T. Underpotential deposition of copper on Pd(100): An electron spectroscopy study[J]. Journal of Electroanalytical Chemistry, 1993, 353(1): 131-145.

[24] Chierchie T, Mayer C. Voltammetric study of the underpotential deposition of copper on polycrystalline and single crystal palladium surfaces[J]. Electrochimica Acta, 1988, 33(3): 341-345.

[25] Park J H, Zhou H J, Percival S J, et al. Open circuit (mixed) potential changes upon contact between different inert electrodes-size and kinetic effects[J]. Analytical Chemistry, 2013, 85(2): 964-970.

[26] Alvarez B, Climent V, Rodes A, et al. Potential of zero total charge of palladium modified Pt(111) electrodes in perchloric acid solutions[J]. Physical Chemistry Chemical Physics, 2001, 3(16): 3269-3276.

[27] Schmidt T J, Markovic N M, Stamenkovic V, et al. Surface characterization and electrochemical behavior of well-defined Pt-Pd{111} single-crystal surfaces: A comparative study using Pt{111} and palladium-modified Pt{111} electrodes[J]. Langmuir, 2002, 18(18): 6969-6975.

[28] Wang J X, Inada H, Wu L J, et al. Oxygen reduction on well-defined core-shell nanocatalysts: Particle size, facet, and pt shell thickness effects[J]. Journal of the American Chemical Society, 2009, 131(47): 17298-17302.

[29] Markovic N M, Gasteiger H A, Ross P N. Oxygen reduction on platinum low-index single crystal surfaces in sulfuric acid solution-rotating ring Pt(hkl) disk studies[J]. Journal of Physical Chemistry, 1995, 99(11): 3411-3415.

[30] Gasteiger H A, Kocha S S, SompalliB, et al. Activity benchmarks and requirements for Pt, Pt-alloy, and non-Pt oxygen reduction catalysts for PEMFCs[J]. Applied Catalysis B: Environmental, 2005, 56(1/2): 9-35.

Nafion 含量与阴离子吸附对于铂单原子层核壳结构催化剂制备的影响

杨莉君[1,2], Dustin Banham[1], Elod Gyenge[2], 叶思宇[1*]

(1. 巴拉德动力系统, 9000 Glenlyon Parkway, Burnaby, 英属哥伦比亚省, 加拿大, V5J 5J8; 2. 化学与生物工程学院, 英属哥伦比亚大学, 2360 East Mall, 温哥华, 英属哥伦比亚省, 加拿大, V6T 1Z3)

摘要： 本实验利用铜的欠电位沉积技术，在旋转圆盘电极上以碳负载的钯纳米颗粒为核，制备铂单原子层核壳结构催化剂. 电化学测试用于表征不同 Nafion 含量的添加对于核壳结构催化剂制备的影响. 实验证明，Nafion 的存在会影响铜的欠电位沉积，铂与铜的置换反应，并决定最终制备的核壳结构催化剂的氧还原催化反应的活性. 当催化剂薄层中 Nafion 的含量低于 5%的时候，添加 Nafion 不但可以帮助催化剂附着在旋转圆盘电极表面，而且可以保证制备的催化剂具有较好的氧还原反应催化活性. 在 H_2SO_4 溶液中，钯纳米颗粒的表面存在特殊的阴离子吸/脱附电化学信号峰，这些信号峰可以用来监测 Nafion 含量对于铂单原子层核壳结构催化剂制备的影响.

关键词： 核壳结构催化剂；氧气还原反应；铜欠电位沉积；Nafion 含量；阴离子吸附